

Dielectric and Raman Studies of $0.935(\text{Bi}_{0.5}\text{Na}_{0.5}\text{TiO}_3) - 0.065\text{BaTiO}_3$ Lead Free Ceramics

H. LIDJICI^{a,b,*}, B. LAGOUN^a AND H. KHEMAKHEM^c

^aLaboratoire d'Étude et Développement des Matériaux Semi-conducteurs et Diélectriques, Université de Laghouat, Route de Ghardaïa, B.P. 37G, Laghouat, Algeria

^bLaboratoire des Matériaux et Procédés, Université de Valenciennes et du Hainaut-Cambrésis, Z.I. du Champ de l'Abbesse, 59600 Maubeuge, France

^cLaboratoire des Matériaux Multifonctionnels et Applications (LMMA), Faculté des Sciences de Sfax, Université de Sfax, B.P. 1171, 3000 Sfax, Tunisia

(Received March 24, 2016; in final form November 17, 2016)

The $0.935(\text{Na}_{0.5}\text{Bi}_{0.5})\text{TiO}_3 - 0.065\text{BaTiO}_3$ lead free ceramic was synthesized by conventional solid state reaction technique. Sintering was done at 1200°C for 4 h in air atmosphere. Dielectric and Raman spectroscopic studies have been performed as a function of temperature from 25 to 450°C . The phase transitions from ferroelectric to antiferroelectric and from antiferroelectric to paraelectric order were observed through the dielectric measurements. Further support for the obtained results was drawn from the Raman spectroscopy measurements.

DOI: [10.12693/APhysPolA.130.1431](https://doi.org/10.12693/APhysPolA.130.1431)

PACS/topics: 81.05.Je

1. Introduction

Piezoelectric ceramics are widely used in electronic devices such as sensors and actuators [1]. Because of their high performance and excellent piezoelectric properties Pb-based $\text{Pb}(\text{Zr},\text{Ti})\text{O}_3$ (PZT) ceramics have dominated the area of application mentioned above. However, environmental issues call for the use of nonhazardous substances for device fabrication. This makes the replacement of PZT ceramics imperative, owing to its high content of toxic lead oxide. Therefore, considerable effort has been devoted to the development of lead-free piezoelectric ceramics with properties comparable to PZT. With the objective of developing of potential advanced lead-free piezoelectric ceramics, compositions are formulated near the morphotropic phase boundary (MPB) between different phases as these generally show superior piezoelectric response. The $(1-x)(\text{Na}_{0.5}\text{Bi}_{0.5})\text{TiO}_3 - x\text{BaTiO}_3$ (abbreviated as NBT- x BT) system was of great interest since the discovery of the MPB at $x = 0.06 - 0.07$ in 1991 by Takenaka et al. [2], where a rhombohedral and a tetragonal symmetries coexist in the system. The interest has arisen largely because the MPB was reported to separate the rhombohedral BNT and the tetragonal BT as in PZT, accompanied by a significant enhancement in the electrical properties [2-4]. This system attracts great attention and continues to be studied as possible lead-free piezoelectric compounds [5-12].

In this paper we report our work on the temperature dependence of dielectric properties of $0.935(\text{Na}_{0.5}\text{Bi}_{0.5})\text{TiO}_3 - 0.065\text{BaTiO}_3$ (abbreviated as NBT-6.5BT) lead free ceramics. There are not an

important number of studies concerning Raman spectroscopy as function of temperature for BNT- x BT system; an analysis with temperature-dependent Raman spectra was also performed.

2. Experimental procedure

The ceramic samples were prepared by solid state sintering from carbonates Na_2CO_3 (reagent grade, Sigma-Aldrich, 99.5%), BaCO_3 (reagent grade, Sigma-Aldrich, 99.0%), and oxides Bi_2O_3 (Aldrich, 99.9%), and TiO_2 (Riedel-dehaen). The powders were weighted respectively according to NBT-6.5BT composition then mixed by planetary milling in ethanol using agate balls as milling media for 1 h. The milled powders were calcined at 825°C for 4 h in air atmosphere. After calcining, the powders were rehomogenised by planetary milling in ethanol using agate balls for 1 h and then isostatically pressed. The compacted samples were sintered at 1200°C for 4 h in air atmosphere. The as-prepared samples were cut in disks shape of 12 mm in diameter and 1 mm in thickness. The crystal structures of sintered ceramics were determined by means of X-ray diffractometer (RIGAKU Miniflex) using $\text{Cu } K_\alpha$ radiation. The microstructure of the sintered ceramics was observed with scanning electron microscope (SEM, HITACHI, S-3500N). The Raman scattering experiments were performed using a micro Raman spectrometer (LABRAM, HR800), working in a back scattering configuration, equipped with a He^+ ion ($\lambda = 633 \text{ nm}$) laser. The spectral resolution of the system was 3 cm^{-1} . Silver electrodes were applied on polished samples to provide good electrical contact. The variation of dielectric constant with temperature at different frequencies was studied from room temperature to 450°C using a computer controlled impedance Analyzer (Agilent 4284A).

*corresponding author; e-mail: hlidjici@yahoo.fr

3. Result and discussion

Figure 1a shows the X-ray diffraction (XRD) pattern of the sintered composition. The XRD pattern was determined by means of X-ray diffractometer (RIGAKU Miniflex) using $\text{Cu } K_{\alpha}$ radiation in the 2θ range of $20\text{--}70^{\circ}$. From Fig. 1a, it can be seen that the sample displays a pure perovskite structure phase. It can be clearly seen that the (003), (021) reflections of rhombohedral phase and (200), (002) reflections of tetragonal phase appear near 39.84° and 46.51° , respectively. This result shows that the sample exhibit co-existence of a rhombohedral-tetragonal phase.

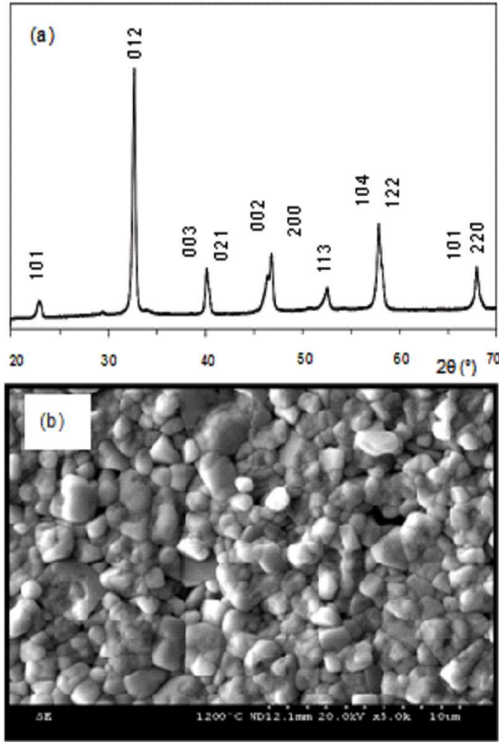


Fig. 1. (a) X-ray diffraction pattern and (b) scanning electron micrograph of the $0.935(\text{Bi}_{0.5}\text{Na}_{0.5})\text{TiO}_3\text{--}0.065\text{BaTiO}_3$ ceramic.

Figure 1b exhibits the SEM micrographs of the prepared ceramic. The average grain size is about 2 to 3 μm . It was reported in literature that for PZT and La^{+3} doped PZT (PLZT) based ceramics, the substitution of Ba^{+2} for Pb^{+2} generally leads to a great inhibition of grain growth [13, 14]. Similar to Ba-modified lead-based ceramics, for the $(1-x)\text{NBT}\text{--}x\text{BT}$ ceramics, grain growth is inhibited after the introduction of BaTiO_3 into $\text{Na}_{0.5}\text{Bi}_{0.5}\text{TiO}_3$ structure.

The relative permittivity ϵ_r and dielectric loss $\tan(\theta)$ of the NBT-6.5BT ceramics are measured from ambient temperature to 450°C with different frequencies. It can be seen that ϵ_r increases with increase in temperature, attains its maximum value at maximum temperature T_m and then decreases (Fig. 2a). This dielectric

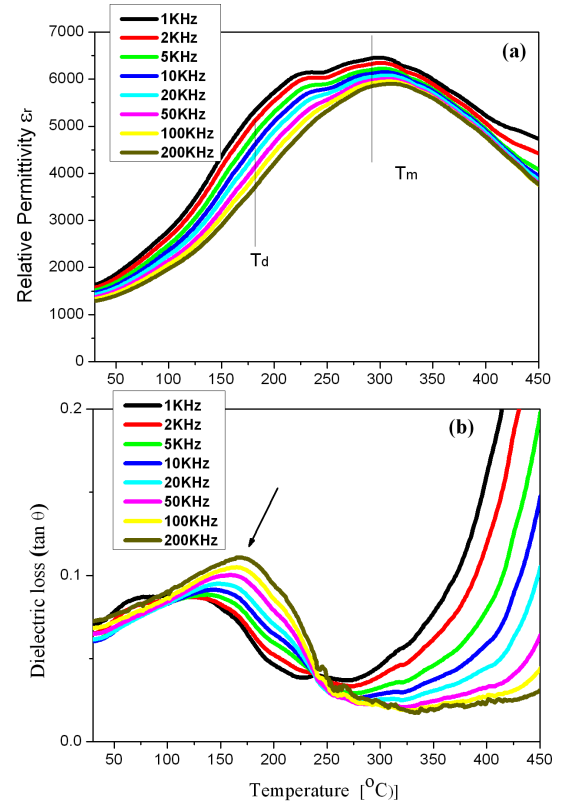


Fig. 2. Variation of (a) relative permittivity (ϵ_r) and (b) dielectric loss as a function of temperature for various frequencies.

anomaly is representing the antiferroelectric–paraelectric phase transition of diffuse nature. It was reported [15] that this maximum may originate from relaxation processes connected with both electrical and mechanical interactions between polar regions and the non-polar matrix, without any structural phase transition. It is also observed that at temperature around 170°C (called depolarization temperature T_d), there is a bifurcation in dielectric constants for different frequencies. This may be due to the ferroelectric to antiferroelectric phase transition. Following Hiruma et al. [16, 17] the depolarization temperatures is defined as the first inflection point in the dielectric loss tangent curves and is labeled with arrow on the dielectric loss tangent curves in Fig. 2b.

TABLE I

The values of T_d and T_m of the present work and for some lead free materials.

| Sample | Our work | NBT-NBZN [18] | NBT-KBT-BT [19] |
|----------------|-----------------------|-----------------------|-----------------------|
| T_d at 1 kHz | 170°C | 210°C | 205°C |
| T_m at 1 kHz | 290°C | 315°C | 300°C |

The dielectric loss $\tan(\theta)$ increases with the increase of temperature particularly beyond 250°C (Fig. 2b). The increase in dielectric loss $\tan(\theta)$ at higher temper-

ature might be due to increased electrical conductivity. The important mechanism of ionic conductivity in this system is the movement of ions which are the current carriers. It has been long known that the alkali ion is a good current carrier in ceramics; therefore this ion plays an important role in the conductivity of NBT ceramics, since the Na^+ ions move easily upon heating, resulting in the increase in conductivity with increasing temperature and conductivity of the sample. The determined T_d and T_m at 1 kHz is 170°C and 290°C , respectively, comparable with other BNT-based materials [18, 19] (see Table I).

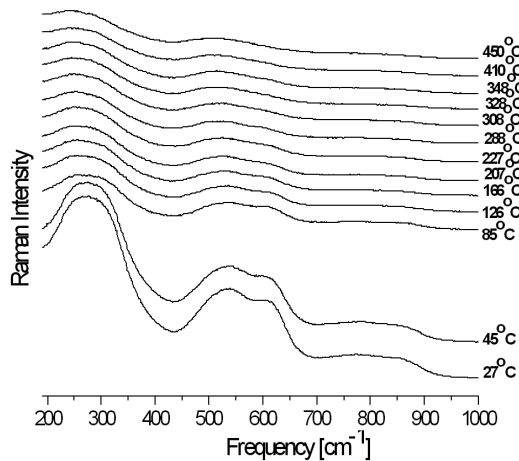


Fig. 3. Temperature dependent Raman-spectra of the $0.935\text{Bi}_{0.5}\text{Na}_{0.5}\text{TiO}_3-0.065\text{BaTiO}_3$ ceramics.

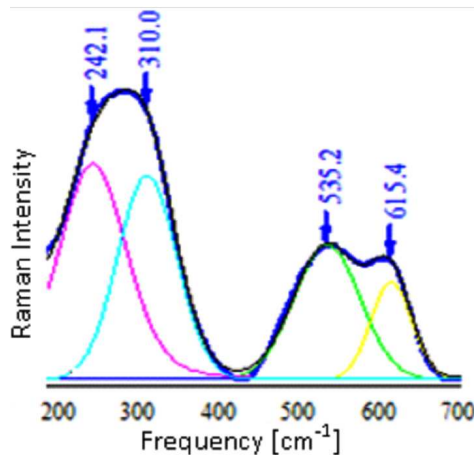


Fig. 4. Fitting of the Raman spectra of $0.935\text{Bi}_{0.5}\text{Na}_{0.5}\text{TiO}_3-0.065\text{BaTiO}_3$ ceramic to the pseudo-Voigt function at room temperature.

In order to confirm the phase transition, temperature-dependent micro-Raman spectra were recorded, as plotted in Fig. 3. Figure 4 represents the Raman spectra of the studied composition at room temperature performed in the range from 200 to 700 cm^{-1} . The deconvolution of the spectrum with LabSpec 5 software using pseudo-Voigt function shows four vibration modes

situated at 242 , 310 , 535 , and 615 cm^{-1} . These results are in good agreement with those reported by Suchanicz et al. [20] and Eerd et al. [21]. The region located between 200 and 400 cm^{-1} is characterized by two lines at 242 and 310 cm^{-1} . For NBT structure, this region is assigned by Ti-O vibration at around 276 cm^{-1} . The studied composition is characterized by the morphotropic phase boundary between rhombohedral and tetragonal phases. This additional line is already considerably seen for the compositions which exhibit the tetragonal phase. It is evident that the arising of the additional line ($\approx 310\text{ cm}^{-1}$) is connected with the appearance of tetragonal symmetry [22].

The modes at 535 cm^{-1} and 615 cm^{-1} are dominated by vibrations involving mainly oxygen displacements. In the measured wave number range, the Raman bands at room temperature are quite broad, which is due to the cation disorder on the 12-fold coordinated site.

Remarkable changes are observed in the Raman spectra with temperature. When temperature reaches 166°C , we can clearly see the abrupt change of the two modes 242 and 310 cm^{-1} in their relative intensity. Considering this result in Fig. 3, we are inclined to attribute the observed change near 166°C to the ferroelectric-antiferroelectric (FE-AFE) phase transition. Furthermore, as temperature is increased, the 615 cm^{-1} mode shifts down and decreases in relative intensity, showing a softening behavior. At 288°C , the mode tends to disappear, and almost overlaps with the 535 cm^{-1} . This indicates the occurrence of antiferroelectric-paraelectric transition [23] which is consistent with results in Fig. 2.

4. Conclusion

In summary, the polycrystalline compound of $0.935(\text{Na}_{0.5}\text{Bi}_{0.5}\text{TiO}_3)-0.065\text{BaTiO}_3$ lead free ceramics has been studied by dielectric and Raman spectra measurements as function of temperature. The dielectric study reveals that the ferroelectric-antiferroelectric phase transition tends to appear near 170°C and the antiferroelectric-paraelectric transition occurs at 290°C . The sequence of phase transitions obtained by dielectric measurements is further verified by thorough Raman spectroscopy analysis.

References

- [1] G.H. Haertling, *J. Am. Ceram. Soc.* **82**, 797 (1999).
- [2] T. Takenaka, K.I. Maruyama, K. Sakata, *Jpn. J. Appl Phys.* **30**, 2236 (1991).
- [3] C. Xu, D. Lin, K.W. Kwok, *Solid State Sci.* **10**, 934 (2008).
- [4] Qing Xu, Shutao Chen, Wen Chen, Sujuan Wu, Joonghee Lee, Jing Zhou, Huajun Sun, Yueming Li, *J. Alloys Comp.* **381**, 221 (2004).
- [5] Qing Xu, Shutao Chen, Wen Chen, Sujuan Wu, Jing Zhou, Huajun Sun, Yueming Li, *Mater. Chem. Phys.* **90**, 111 (2005).

- [6] Brianti Satrianti Utami, Cheng-Nan Chen, Chen-Chia Chou, *Ceram. Inter.* **39**, 175 (2013).
- [7] G. Picht, J. Töpfer, E. Hennig, *J. Eur. Ceram. Soc.* **30**, 3445 (2010).
- [8] Xiu-Cheng Zheng, Guang-Ping Zhengn, Zheng Lin, Zhi-Yuan Jiang, *Ceram. Int.* **39**, 1233 (2013).
- [9] D.K. Sharma, N. Kumar, S. Sharma, R. Rai, *Mater. Chem. Phys.* **141**, 145 (2013).
- [10] H. Foronda, M. Deluca, E. Aksel, J.S. Forrester, J.L. Jones, *Mater. Lett.* **115**, 132 (2014).
- [11] H. Lidjici, M. Rguiti, F. Hobar, C. Courtois, A. Leriche, *Mater. Sci.-Poland* **29**, 9 (2011).
- [12] H. Lidjici, H. Khemakhem, *Ceram.-Silik.* **60**, 205 (2016).
- [13] K. Ramam, M. Lopez, *J. Phys. D Appl. Phys.* **39**, 4466 (2006).
- [14] K. Ramam, S.H. Luis, *Phys. Status Solidi A* **203**, 2119 (2006).
- [15] G.O. Jones, P.A. Thomas, *Acta Crystallogr. B Struct. Sci.* **58**, 168 (2002).
- [16] Y. Hiruma, H. Nagata, T. Takenaka, *Jpn. J. Appl. Phys.* **45**, 7409 (2006).
- [17] Y. Hiruma, H. Nagata, T. Takenaka, *J. Appl. Phys.* **104**, 124106 (2008).
- [18] Xin-Yu Liu, Chang-Rong Zhou, Zhao-Hui Shan, *Bull. Mater. Sci.* **30**, 579 (2007).
- [19] Y.M. Li, W. Chen, Q. Xu, J. Zhou, X. Gu, S. Fang, *Mater. Chem. Phys.* **94**, 328 (2005).
- [20] J. Suchanicz, I. Jankowska-Sumara, T.V. Kruzina, *J. Electroceram.* **27**, 45 (2011).
- [21] B. Wylie-van Eerd, D. Damjanovic, N. Klein, N. Setter, J. Trodahl, *Phys. Rev. B* **82**, 104112 (2010).
- [22] B. Parija, T. Badapanda, S. Panigrahi, T.P. Sinha, *J. Mater. Sci. Mater. Electron.* **24**, 402 (2013).
- [23] J. Petzelt, S. Kamba, J. Fabry, D. Noujni, V. Porokhonsky, A. Pashkin, I. Franke, K. Roleder, J. Suchanicz, R. Klein, G.E. Kugel, *J. Phys. Condens. Matter* **16**, 2719 (2004).